On Measurement Uncertainty of a Vortex Flowmeter

Jiun-Jih J. Miau[1,2], Chen-Fan. Yeh[1], Chih-Chung Hu[1,2], and Jung-Hua Chou[3]

([1]Department of Aeronautics and Astronautics, National Cheng Kung University, Tainan, Taiwan, China)

([2]Aerospace Science and Technology Research Center, National Cheng Kung University, Tainan, Taiwan, China)

([3]Department of Engineering Science, National Cheng Kung University, Tainan, Taiwan, China)

Abstract Measurement uncertainty of a T-shaped flowmeter was examined with a gas flow calibration facility, for Reynolds numbers, Re_d, in a range of 2.56×10^4-1.56×10^5. The total uncertainty interval of the Strouhal values deduced from a Fourier spectral analysis was ±0.745%, and the linearity of the data was ±1.78%. Meanwhile, a scheme based on pulses counting in reference to the analog signals measured gave the total uncertainty interval of the meter factor as ±0.568%, with the linearity ±1.89%.

Keywords: Vortex flowmeter; Measurement uncertainty

1. Introduction

Despite that the measurement principle of vortex flowmeter is straightforward and simple, practically the performance of a vortex flowmeter is concerned greatly with its rangeability and measurement uncertainty. It is logical to regard a vortex flowmeter as a system. The system consists of a vortex shedder to induce shedding vortices, a sensor detecting the vortex shedding signal, and a data processing unit to compute and display the flow rate measured. To improve the performance of a vortex flowmeter, one has to tackle various issues in conjunction with the components indicated above.

This study was intended to explore the measurement uncertainty of a T-shaped vortex flowmeter developed in the laboratory as it being tested in a gas flow calibration facility.

2. Experimental Facility

The vortex flowmeter employed is featured with a T-shaped vortex shedder, shown in Fig.1.[1] The diameter is 150mm, denoted as d, in this paper. A piezoelectric sensor was hard-bounded in the middle of the extended plate of the shedder for detecting the vortex shedding signal,[2] seen also in the figure. The output signals could be analyzed by an analog circuit for pulses counting, or converted into a digital format to be processed by computer software.

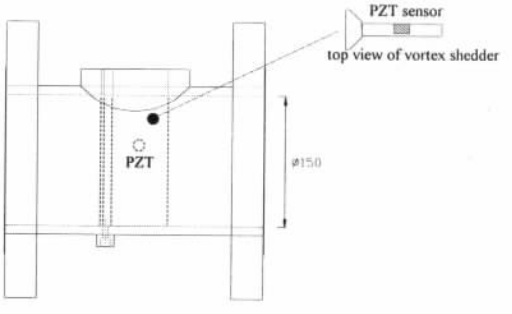

Fig.1 A schematic drawing of the vortex flowmeter of 150mm in diameter.

The gas flow calibration facility employed for the present study receives upstream compressed air at pressure up to 50 bars. An array of regulators designated for different ranges of flow rates are situated immediately downstream of the inlet of the system to ensure the downstream air pressure at a preset value. The pipe flow is choked by a set of standard nozzles, such that the mass or volume flow

rate can be calculated according to the gas dynamics relations with the pressure and temperature immediately upstream of the nozzles known.

In the facility, the volume flow rate ranges from 10 to 2.4×10^4 m^3/hr at the atmospheric pressure. The system uncertainty is ±0.31%, certified by CNLA (Chinese National Laboratory Accreditation).

3. Data Reduction Schemes

The vortex shedding frequency of interest is frequently expressed in the non-dimensional form as follows.

$$St = \frac{f \cdot W}{V} \qquad (1)$$

where St, f, W, and V denote the Strouhal number, the vortex shedding frequency measured, the width of the vortex shedder and the bulk velocity, respectively. W is assumed to be fixed in the present framework. During the experiment, the output signals of the sensor were sampled at the rate of $10^3 Hz$, for which 18 data blocks were taken continuously at a fixed flow rate. In this study, each data block had 4096 points, which was then analyzed by Fourier transform to obtain the vortex shedding frequency. As the mean volume flow rate within the time of a block of data was obtained according to the pressure and temperature upstream of the standard nozzles, the Strouhal number for each block of data could be reduced. Based on this data reduction scheme, the standard deviation associated with the Strouhal values obtained from the 18 data blocks can be deduced, denoted as $s(St)$. Further, the standard deviation corresponding to the mean Strouhal value, denoted as $s(\overline{St})$, can be determined as follows. [3]

$$s(\overline{St}) = \frac{s(St)}{\sqrt{n}} \qquad (2)$$

In (2), $n=18$ denotes the number of the blocks employed in data reduction, where $\overline{St}$ denotes the mean Strouhal value of the 18 values. Consequently, the uncertainty due to repeatability of $\overline{St}$, denoted as U_1, can be determined as

$$U_1 = 2 \cdot [\frac{s(\overline{St})}{\overline{St}}] \qquad (3)$$

The tests were repeated in six different days. Therefore, for each flow rate perofrmed, six values of $\overline{St}$ were obtained, the corresponding mean value, $\overline{\overline{St}}$, and standard deviation, $s(\overline{\overline{St}})$, were calculated. Subsequently, the uncertainty due to reproducibility of $\overline{\overline{St}}$, denoted as U_2, was determined according to the following expression.

$$U_2 = 2 \cdot [\frac{s(\overline{\overline{St}})}{\overline{\overline{St}}}] \qquad (4)$$

In addition to U_1 and U_2, frequency resolution in spectral analysis and uncertainty of the flow calibration system are two other possible sources contributing to the total uncertainty of St. Hence, at least four sources of uncertainties were associated with the Strouhal value reduced; namely

$$U_{St}^2 = U_1^2 + U_2^2 + U_3^2 + U_4^2 \qquad (5)$$

In specific,

U_{St}: total uncertainty of Strouhal value;

U_1: repeatability;

U_2: reproducibility;

U_3: uncertainty of resolution in spectral analysis;

U_4: uncertainty of the flow calibration system.

Note that U_{St} and U_1-U_4 denote the expanded uncertainties [3], each of which is referred to the 95% confidence interval. Since each block of 4096 data points is chosen for the Fourier analysis, the frequency resolution in the spectral results is about 0.25 Hz. Thus, U_3 is determined as the ratio of 0.25 Hz to the vortex shedding frequency read from the spectral results. Clearly, the higher the vortex shedding frequency or the longer the length of a block of the data, the lower the uncertainty of U_3.

The piezoelectric sensor signals were processed by an

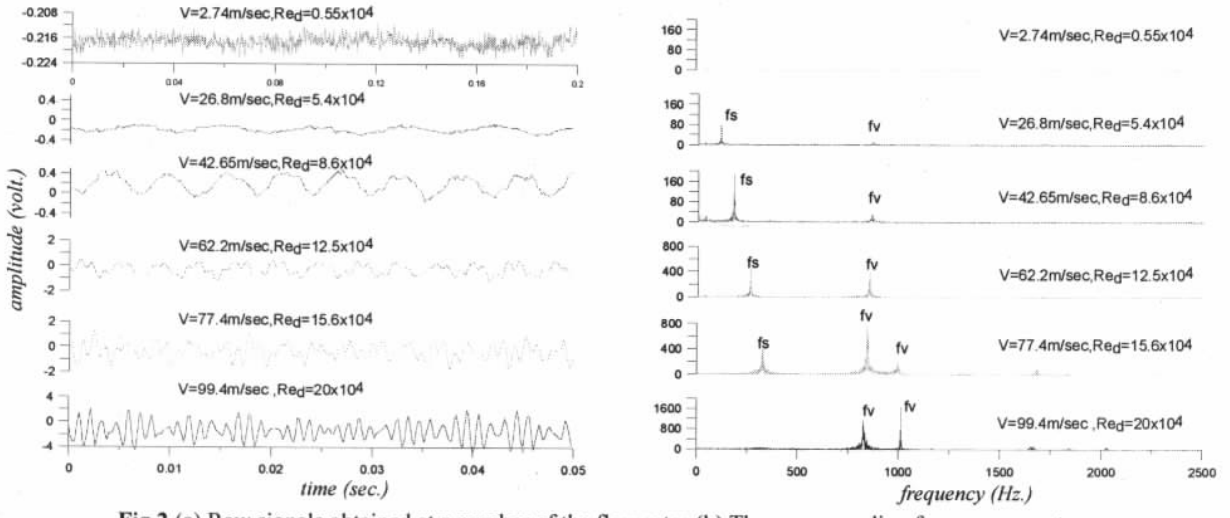

Fig.2 (a) Raw signals obtained at a number of the flow rates.(b) The corresponding frequency spectra.

analog circuit separately. The volume flow rate could be reduced in terms of a K factor defined.

$$K = \frac{pulse\_number}{volume\_flow} \tag{6}$$

Hence, the total uncertainty of the K factor, denoted as U_k, can be expressed as follows.

$$U_k^2 = U_1^2 + U_2^2 + U_3^2 + U_4^2 \tag{7}$$

Note that in this expression, the quantity U_3 is due to the uncertainty of pulses counting over the time sampled. Since in the measurement, at least 10,000 pulses were counted for reducing a K factor value, this uncertainty basically was less than 0.01%. Therefore, the uncertainty is rather small compared to the other terms in (7), hence can be neglected. The raw signals obtained at a number of the flow speeds are presented in Fig.2a. Moreover, the corresponding frequency spectra are given in Fig.2b for reference. From these plots, one realizes that the vortex shedding frequency can not be disernable at the lowest Reynolds number shown, $Re_d = 0.55\times10^4$, where Re_d denotes the Reynolds number based on d and V. As V is increased, two frequency components other than the vortex shedding frequency gets pronounced, indicated by f_v in the spectral plots, which appear to be invariant with the flow velocity. As confirmed by the output signals of an accelerometer placed on the piping structure, these components were due to structural vibrations. At V=99.4 *m/s*, the structural vibrations appear to dominate over the vortex shedding component in sensor signals measured, thus identification of the vortex shedding frequency becomes impossible. Consequently, the present measurements of vortex shedding frequency were limited in the range of V=12.72-77.6*m/s*, equivalent to Re_d = 2.56×10^4-1.56×10^5.

4. Analysis of Measurement Uncertainty

Fig.3 presents the results of St versus the Reynolds numbers studied. In the figure, every six "▲" symbols of about the same flow rate are clustered around a "×" symbol, where each of the "▲" symbols indicates a $\overline{St}$ value obtained and the "×" symbol indicates the resultant $\overline{\overline{St}}$ value. A 6th-order polynomial function was used to fit the "×" symbols, shown by a solid curve in Fig.3. The uncertainty level of the solid curve in reference to the experimental data can be evaluated as follows.

$$U_{St\_ref}^2 = U_{St}^2 + U_5^2 \tag{8}$$

where U_{St_ref} denotes the uncertainty of the curve fitting and U_5 refers to the deviation of the Strouhal

value $\overline{St}$ from the curve fitting. The total uncertainty intervals of U_{St_ref} deduced are ±0.748% and ±0.854% indicated by two pairs of dashed curves. Note that the uncertainty interval of U_{St_ref} = ±0.748% is deduced with U_1 taken as the average of the standard deviations, $s(\overline{St})$, obtained in six different days; whereas the uncertainty interval of U_{St_ref} = ±0.854% is deduced with U_1 taken as the largest among the standard deviations obtained in six different days.

The "o" symbols in Fig.3 show the data points of $\overline{St}$ values obtained afterwards to validate the uncertainty intervals of U_{St_ref} shown. These proof data appear to fall within the total uncertainty intervals of U_{St_ref}, hence give a direct support to the relevance of (8). If there were other major uncertainty sources not included in (8), some of the proof data points would have been fallen outside the uncertainty intervals of U_{St_ref}.

Fig.4 shows the individual contributions of U_1, U_2, U_3, and U_5 to the total uncertainty, U_{St_ref}, at the five flow rates studied. First of all, it is seen that higher measurement uncertainty is resulted at lower volume flow rate. In fact, the total uncertainty interval of U_{St_ref} = ±0.854% or ±0.748% shown in Fig. 3 were deduced in reference to the data obtained at the volume flow rate 1212 m^3/hr, which is the largest among those of the five volume flow rates tested. Secondly, among the uncertainty sources, U_1 associated with repeatability is always noticeable regardless of the flow rates. On the other hand, U_2 associated with reproducibility appears to be less significant. Thirdly, the contribution of U_3 gets less important as the flow rate gets increased. This is plausible, since the frequency resolution of the present spectral analysis is invariant with respect to V, but the vortex shedding frequency gets increased with V. Based on the observations above, one can say that an effective strategy to improve the measurement uncertainty of U_{St_ref} would be to reduce U_1. Hence, one might have to look into the possibilities of improving the stability of vortex shedding or the design of the sensor. The other strategy would be to improve the frequency resolution of the spectral analysis, especially when flow rate is low. Implementation of this strategy would imply an increase of the sampled time, if the number of the blocks is kept the same.

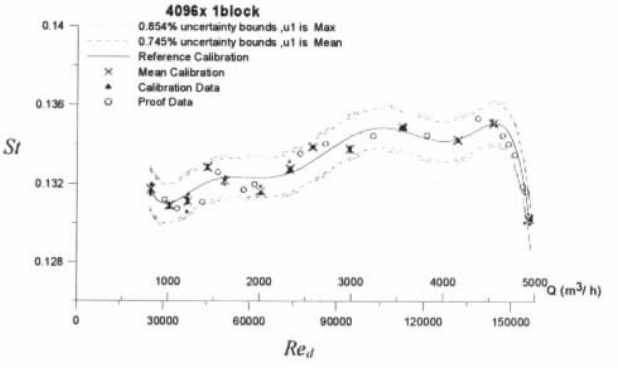

Fig.3 Strouhal values versus the flow rates tested in the gas flow calibration system.

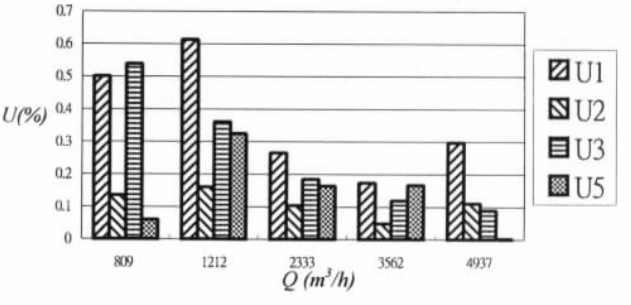

Fig.4 Comparison of the uncertainty contributions at the five flow rates tested in the gas flow calibration facility.

Fig.5 presents the variations of the K factor with respect to the flow rates tested, based on the same sensor signals as those led to Fig.3. Similarly, in this figure, two pairs of the curves indicating the total uncertainty intervals of U_{K_ref} correspond to U_1 reduced according to as the maximum value of $s(\overline{K})$ among the values obtained in six different days, and U_1 reduced according to the mean of the $s(\overline{K})$ values obtained, respectively. The uncertainty intervals are ±0.577% and ±0.568%, which are notably less than

the U_{St_ref} intervals in Fig.3. The difference is mainly due to that U_3 was negligible in computing U_{K_ref}, mentioned earlier. Referring to Fig.4, one can see that as flow rate gets higher, U_3 gets less significant, consequently the total uncertainty interval of U_{St_ref} becomes comparable to U_{K_ref}.

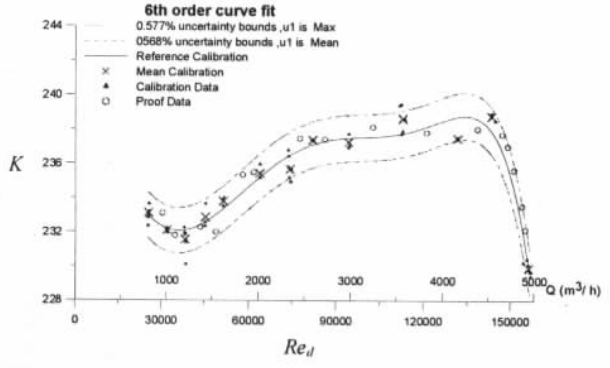

Fig.5 K values versus the flow rates tested in the gas flow calibration system.

The symbols "×", "▲", and "o" in Fig.5 bear the same meanings as those shown in Fig.3. It is also worthwhile to mention that all the proof data points indicated by the symbols "o" fall within the total uncertainty intervals of U_K defined.

Also noted in Figs.3 and 5 is that the distributions of $\overline{St}$, $\overline{\overline{St}}$, $\overline{K}$, and $\overline{\overline{K}}$ values show significant non-linearity at Re_d around 1.5×10^5. The trend of drastic variations is further confirmed by several proof data points shown in the figure, whose flow rates fall in the vicinity of $Re_d=1.5\times10^5$. As the data points indicate the trend consistently, one realizes that the non-linearity is an intrinsic characteristic of the present flowmeter in the range of the Reynolds numbers studied. Following the ASME standard[4], a quantitative description on the non-linear behavior of the St-Re_d relation can be given in terms of the linearity defined below.

$$\text{Linearity } (St)=\frac{\overline{St}_{\max}-\overline{St}_{\min}}{2\overline{\overline{St}}_{mean}} \qquad (9)$$

where $\overline{\overline{St}}_{mean}=\dfrac{\overline{St}_{\max}+\overline{St}_{\min}}{2}$

In (9), the subscripts "max" and "min" denotes the maximum and minimum values seen in Fig.3. Hence, the linearity corresponding to the $\overline{\overline{St}}$ values indicated by the symbols "×" in Fig.3 is found ±1.78%. Similarly, the linearity corresponding to the $\overline{\overline{K}}$ values indicated by the symbols "×" in Fig.5 is found ±1.89%.

5. Discussion

Further discussion on the linearity of the St-Re_d relation is made here. Referring to the literature[5], it is known that for a uniform flow over a bluff body, the characteristics of the wake flow, such as, base pressure, vortex formation length and vortex shedding frequency, appear to be sensitive to Reynolds numbers in specific ranges. In Corpron[6], the data concerning the performance of a T-type cross section vortex flowmeter revealed that the meter factor values reduced were in fact varied substantially over a range of Reynolds numbers of 10^4-10^7. Hence, the non-linearity as an intrinsic behavior of the St-Re_d relation over a wide range of Reynolds numbers is well recognized. Also, the non-linearity varies with a number of the parameters, for instance, the configuration of the vortex shedder[7,8], freestream turbulence intensity[9], and so on. Physically speaking, the non-linearity could be involved with the three-dimensionality of vortex shedding[10,11]. These complicated flow phenomena are sensitive to Reynolds number. Based upon the understandings above, in practical application one might look for a proper shape of the vortex shedder to avoid severe non-linearity in the measured flow range, thus the flow rate could be converted from the vortex shedding frequency measured with a linear relation simply. Otherwise, one has to face the issue of non-linearity,

which might affect the accuracy of flow measurement considerably. Along this consideration, more complicated data reduction scheme would be necessary[12].

6. Conclusions

This study conducted a serious of tests of a vortex flowmeter in a gas flow calibration facility. In the range of Re_d=2.56×10^4-1.56×10^5, the total uncertainty intervals of the flowmeter deduced by the Fourier transform analysis and the analog circuit are ±0.745% and ±0.568%, respectively. The discrepancy is attributed to that in the spectral analysis the uncertainty associated with frequency solution has to be included into consideration. Also noted, the total uncertainty is significantly contributed by the component of repeatability. The proof data points shown in Figs.3 and 5 validate the expressions of (8) that the total uncertainties can be estimated with the components of U_1-U_5. Noticeable non-linearity is found in both of St-Re_d and K-Re_d relations for Re_d in the vicinity of 1.5×10^5. The linearity factors reduced accordingly are ±1.78% and ±1.89%, respectively.

Acknowledgment

This work was supported by National Science Council, Taiwan, China, under the contract number NSC 91-2212-E-006-046.

References

[1]Miau J. J., Yang C. C., Chou J. H., and Lee K. R., A T-shaped vortex shedder for a vortex flowmeter. Flow Measurement and Instrumentation, 4(4), 1993, 259-267.

[2]Miau J. J., Hu C. C., and Chou J. H., Response of a vortex flowmeter to impulsive vibrations. Flow Measurement and Instrumentation, 11, 2000, 41-49.

[3]ISO Guide to the Expression of Uncertainty in Measurement, 1993.

[4]*Measurement of fluid flow in pipes using vortex flowmeters.* ASME MFC-6M-1998, ASME, 1998.

[5]Roshko A., Perspectives on bluff body aerodynamics. Journal of Wind Engineering and Industrial Aerodynamics, 49, 1993, 79-100.

[6]Corpron G. P., Vortex flowmenter performance characteristics-Part A: The effect of installation conditions on the performance of a T-cross section vortex flowmeter. In *Experimental Uncertainty in Fluid Measurements,* FED-Vol. 58, ASME, 1987.

[7]Igarashi T., Fluid Flow Around a Bluff Body Used for a Karman Vortex Flowmeter. "FLUCOME"85, Proceedings of the International Symposium, Tokyo, 1985, 1003-1008.

[8]Hans V., Poppen G., Lavante E., and Perpeet S., Vortex shedding flowmeters and ultrasound detection: signal processing and influence of bluff body geometry. Flow Measurement and Instrumentation 9, 1998, 79-82.

[9]Wolochuk M. C., Plesniak M. W., Braun J. E., The effects of turbulence and unsteadiness on vortex shedding from sharp-edged bluff bodies. Journal of Fluids Engineering, 118, 1996, 18-25.

[10]Gerrard J. H., The three-dimensional structure of the wake of a circular cylinder. Journal of Fluid Mechanics, 25(1), 1966, 143-164.

[11]Williamson C. H. K., Three-dimensional wake transition. Journal of Fluid Mechanics, 328, 1996, 345-407.

[12]Takahashi S. and Itoh I., Intelligent vortex flowmeter. FLOMEKO'93, Proceedings of the 6th International Conference on Flow Measurement, Korea, 1993, 107-113.